Na^+ Occupancy and Mg^{2+} Block of the *N*-methyl-D-aspartate Receptor Channel

Yongling Zhu and Anthony Auerbach

From the Department of Physiology and Biophysics, State University of New York at Buffalo, Buffalo, New York 14214

ABSTRACT The effect of extracellular and intracellular Na^+ on the single-channel kinetics of Mg^{2+} block was studied in recombinant NR1-NR2B NMDA receptor channels. Na^+ prevents Mg^{2+} access to its blocking site by occupying two sites in the external portion of the permeation pathway. The occupancy of these sites by intracellular, but not extracellular, Na^+ is voltage-dependent. In the absence of competing ions, Mg^{2+} binds rapidly ($>10^8$ $M^{-1}s^{-1}$, with no membrane potential) to a site that is located 0.60 through the electric field from the extracellular surface. Occupancy of one of the external sites by Na^+ may be sufficient to prevent Mg^{2+} dissociation from the channel back to the extracellular compartment. With no membrane potential; and in the absence of competing ions, the Mg^{2+} dissociation rate constant is >10 times greater than the Mg^{2+} permeation rate constant, and the Mg^{2+} equilibrium dissociation constant is ~12 μM. Physiological concentrations of extracellular Na^+ reduce the Mg^{2+} association rate constant ~40-fold but, because of the "lock-in" effect, reduce the Mg^{2+} equilibrium dissociation constant only ~18-fold.

KEY WORDS: ion binding sites • magnesium • channel blockade • permeation • selectivity

INTRODUCTION

At synapses, the channel domain of the *N*-methyl-D-aspartate receptor (NMDAR)[1] interacts with several different metal cations, including Na^+, K^+, Ca^{2+}, and Mg^{2+}. These interactions have important physiological consequences. Activation of NMDARs depolarizes dendrites, with Na^+ and K^+ carrying the bulk of the current. Ca^{2+} entry into dendrites via NMDARs regulates synaptic strength and plasticity (Maren and Baudry, 1995; Asztely and Gustafsson, 1996). Voltage-dependent Mg^{2+} block of NMDARs may allow these receptors to respond specifically to contemporaneous excitatory inputs and, thus, serve as a substrate for Hebbian learning. Given such critical functions, it is likely that the NMDAR has specific structures that govern the passage of Na^+, K^+, Ca^{2+}, and Mg^{2+} through its ion permeation pathway.

These four cations interact with the NMDAR protein over time scales that span more than four orders of magnitude. Na^+ and K^+ are highly permeable and pass through the pore rapidly. In symmetric, 100-mM divalent cation-free solutions, the NMDAR conductance is ~70 pS for both of these ions, which means that at −60 mV, Na^+ and K^+ interact with the channel for <0.04 μs. The contact between these ions and the protein is too brief to be resolved as discrete events in the single-channel record. Instead, the interaction of Na^+ and K^+ with the NMDAR pore has been probed mainly using current-voltage relationships (Mayer et al., 1984; Nowak et al., 1984; Cull-Candy and Usowicz, 1987) and by measuring their effects on channel block (Chen and Lipton, 1997; Antonov et al., 1998; Antonov and Johnson, 1999).

Under physiological conditions, ~10–15% of the NMDAR current is carried by Ca^{2+} (Burnashev et al., 1995). This divalent cation moves through the wild-type (NR1-NR2B) channel ~100 times more slowly than Na^+, i.e., with a rate constant of ~10^6 s^{-1} (Premkumar and Auerbach, 1996). Thus, Ca^{2+} resides in the permeation pathway for ~1 μs. Information regarding Ca^{2+} transmission has been derived mainly from measurements of macroscopic currents (Mayer and Westbrook, 1987; Iino et al., 1990; Jahr and Stevens, 1993; Sharma and Stevens, 1996b), single-channel currents (Iino et al., 1997), or fluxes (Burnashev et al., 1995). However, certain mutations reduce the Ca^{2+} permeation rate constant to such an extent that its binding and unbinding are manifest as excess open channel noise (Premkumar and Auerbach, 1996).

Mg^{2+} is the slowpoke of the group. This divalent cation typically dwells in the pore for >100 μs (Ascher and Nowak, 1988; Jahr and Stevens, 1990). Occupancy of the channel by one Mg^{2+} eliminates conduction by other ions and generates a discrete gap in the single-channel current record. Therefore, the microscopic

Address correspondence to Anthony Auerbach, Department of Physiology and Biophysics, School of Medicine and Biomedical Sciences, SUNY at Buffalo, 124 Sherman Hall, Buffalo, NY 14214. Fax: (716) 829-2569; E-mail: auerbach@buffalo.edu

[1]*Abbreviations used in this paper:* MSC, model selection criterion; NMDAR, *N*-methyl-D-aspartate receptor.

rate constants for Mg^{2+} entry and exit from the pore can be determined readily using single-channel kinetic techniques (Ascher and Nowak, 1988).

The compositions, characteristics, and locations of the important sites of ion interaction in the NMDAR permeation pathway are not completely understood. Mg^{2+} binds to a site that is (in electric distance) about half way through the channel (Wollmuth et al., 1998; Antonov and Johnson, 1999). This site is formed, in part, by an asparagine residue in the M2 (pore-forming) segment of the NR2 subunit (Wollmuth et al., 1998), although mutations of other M2 residues also influence Mg^{2+} blockade (Burnashev et al., 1992; Sharma and Stevens, 1996a). Ca^{2+} binds to a site that is distinct from the Mg^{2+} binding site and that may lie at the extracellular margin of the electric field of the membrane (Premkumar and Auerbach, 1996; Sharma and Stevens, 1996b). Na^+ interacts with two sites that are also located at the extracellular limit of the electric field (Antonov et al., 1998). The residues that constitute the Ca^{2+} and Na^+ binding sites have not been clearly identified. In addition, almost nothing is known about the key sites of interaction for K^+ in the NMDAR channel.

The vast difference in residence times for Na^+ and K^+ versus Mg^{2+} in the NMDAR channel is such that there are on the order of 10^4 monovalent cation-binding/unbinding events for each Mg^{2+} binding event. Accordingly, the occupancy by monovalent cations is in steady state on the time scale of Mg^{2+} blockade. The locations and affinities of the binding sites for these mobile ions can be probed by measuring the effect of the extra- and intracellular concentrations of Na^+ and K^+ on the kinetics of Mg^{2+} block. This approach has been used to probe permeant ion binding sites in native NMDARs (Antonov et al., 1998; Antonov and Johnson, 1999).

In this and in the companion paper (see Zhu and Auerbach, 2001, in this issue), we present a single-channel analysis of the effects of extra- and intracellular Na^+ and K^+ on the kinetics of Mg^{2+} block of recombinant NR1-NR2A NMDAR. The results suggest that Na^+ mainly interacts with two sites that are located external to the site of Mg^{2+} blockade, whereas K^+ interacts with these sites plus an additional site located near the intracellular margin of the electric field. We extrapolate the results to estimate the kinetics, affinity, and voltage dependence of Mg^{2+} block in the absence of competing ions.

MATERIALS AND METHODS

Expression of NMDAR in Xenopus Oocytes

Wild-type rat cDNA for the NR1 (splice variant 1) and NR2A subunits were provided by Dr. Thomas Kuner and Dr. Peter Seeburg (Max-Planck Institute for Medical Research, Heidelberg, Germany). These two subunits were coexpressed in *Xenopus* oocytes by injection of 50 nl each of cRNA (1 μg/ml). Electrophysiology experiments were performed 3–10 d after injection. A more detailed description of the molecular biology and expression protocols is given in Premkumar and Auerbach (1996).

Electrophysiology and Solutions

Single-channel currents were recorded from outside-out patches. Recording pipets were pulled from borosilicate glass (World Precision Instruments) and were coated with Sylgard (Dow Corning). The pipet resistance was 10–15 MΩ. Patch pipets were filled with the following reagents (in mM): 5–100 NaCl, 2 K_2ATP, 1 BAPTA, 0.25 GTP, and 10 HEPES, pH adjusted to 7.3. The extracellular solution contained 50 μM NMDA, 10 μM glycine, 2.5 mM KCl, 5 mM HEPES, and 1.5 mM EDTA (pH adjusted to 7.3) plus added NaCl, KCl, and $MgCl_2$ (ultrapure grade from Johnson Mattey). BAPTA, EDTA, HEPES, and all other salts were obtained from Sigma-Aldrich. Without compensation by other ions, the amount of NaCl or KCl was adjusted to achieve the desired Na^+ or K^+ concentration. Using the parameters estimated by the program MAXC, the desired free Mg^{2+} concentrations were established by adding the calculated amount of $MgCl_2$ to solutions buffered with EDTA (1.5 mM) as the Mg^{2+} chelator. Here, we report $[Mg^{2+}]$ as a concentration rather than an activity. Glucose was added to the extracellular solution or pipet solution to balance the osmolarity. The junction potentials between the pipet solution and the extracellular solution were calculated and the membrane potential was corrected accordingly (Barry and Lynch, 1991). All experiments were performed at 22–25°C. Upon excision of patches in the outside-out configuration, an ALA BPS-4 perfusion system (ALA Scientific Instruments) controlled the exchange of experimental and control solutions.

Signal Processing

The currents were recorded using a patch-clamp amplifier (model EPC-7; Medical-Systems-List). The currents were low-pass filtered at 10 kHz, sampled at 94 kHz using a data recorder (model VR-10B; Instrutech Corp.), and stored on videotape. Recorded currents were stored on a PC at sampling frequency of 94 kHz using a VR-111 interface (Instrutech Corp.).

Kinetic Analysis

To study the kinetic properties of Mg^{2+} block, it was necessary to distinguish the blocked state from the other nonconducting (closed) states. In the absence of Mg^{2+}, NR1-NR2A receptors have two main conductance levels: open and closed (Fig. 1 A, top trace). There were usually two components in the open interval lifetime distribution (0.1 ms, 29%; and 5 ms, 71%; data not shown) and at least three components in the closed interval lifetime distribution (0.5 ms, 22%; 7 ms, 12%; and a duration >40 ms that varied with the agonist concentration; data not shown). The addition of Mg^{2+} to the extracellular solution induces frequent, brief gaps (Fig. 1 A, middle and bottom traces) that reflect the binding and unbinding of Mg^{2+} to the NMDAR channel.

The kinetics of Mg^{2+} block were quantified using the QuB software suite (www.qub.buffalo.edu). First, closed-channel events longer than 3 ms were discarded (program PRE, version 1.2.0.0). The remaining segments of current were digitally low-pass filtered (f_c = 5 kHz; final signal f_c = 4.5 kHz) and idealized using a recursive Viterbi algorithm (program SKM; version 1.1.0.000; Chung et al., 1990). From the idealized current level sequences, rate constants were estimated using a maximum interval likelihood approach that included a first-order correction for missed events (MIL; version 2.0.6.000; Qin et al., 1996). Typically, a dead time of 50 μs was imposed. Events shorter than this time were concatenated with the adjacent intervals. To account for a short-lived component of channel closure (as distinct from Mg^{2+}

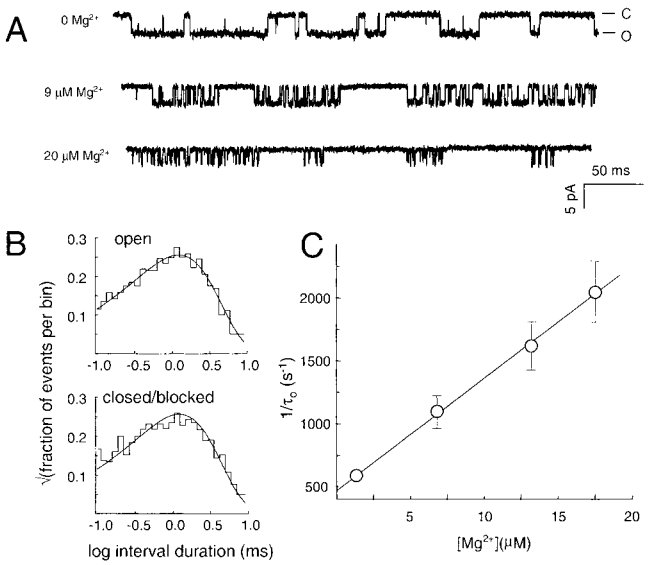

FIGURE 1. Block of NR1-NR2A NMDA receptors by extracellular Mg^{2+}. (A) Single-channel currents from NR1-NR2A NMDA receptors recorded from outside-out patches in the absence and presence of extracellular Mg^{2+}. Currents were activated by 50 μM NMDA and 10 μM glycine, and the membrane potential was −80 mV. Both the extracellular and intracellular solutions contained 100 mM Na^+. Openings are shown as downward deflections. (B) Interval duration histograms (9 μM Mg^{2+}). In this example, the inverse of the mean open time was 917 s^{-1}, and the inverse of the mean block time was 901 s^{-1}, which is the net rate of Mg^{2+} release from the pore (k_{off}) either by dissociation back to the extracellular solution or permeation into the intracellular solution. (C) The inverse of the open interval lifetime (τ_o) versus the extracellular [Mg^{2+}]. Each point is the mean ± SD from at least three patches (in some cases, the SD is smaller than symbol). The Mg^{2+} association rate constant is the slope of this relationship (89.0 ± 2.2 $\mu M^{-1}s^{-1}$; mean ± SD).

blockade), interval durations were fitted by a three-state (C_1-O_2-C_3) model. Thus, any fast closures that were included along with the blocking gaps were explicitly taken into account. Density functions calculated from the fitted rate constants were superimposed upon interval duration histograms to provide a visual check of the accuracy of the fit (Fig. 1 B). The open channel lifetime was defined as the time constant of the slower, predominant component of the open interval duration distribution.

We used the following kinetic model (Scheme 1) to describe the transitions between open and blocked states:

$$\text{pore} + \text{extracellular } Mg^{2+} \underset{k_{-Mg}}{\overset{k_{+Mg}[Mg^{2+}]_{ex}}{\rightleftharpoons}} \text{pore-}Mg^{2+} \xrightarrow{k_{pMg}} \text{pore} + \text{intracellular } Mg^{2+} \quad \text{(SCHEME I)}$$

where k_{+Mg} is the extracellular Mg^{2+} association rate constant, $[Mg^{2+}]_{ex}$ is the extracellular [Mg^{2+}] concentration, k_{-Mg} is the Mg^{2+} dissociation rate constant (i.e., back to the extracellular solution), and k_{pMg} is the Mg^{2+} permeation rate constant (i.e., into the intracellular compartment). k_{+Mg} is related to the channel open lifetime (τ_o) by:

$$\frac{1}{\tau_o} = \alpha + k_{+Mg}[Mg^{2+}]_{ex},$$

where α is the intrinsic channel closing rate constant. Thus, the inverse of the channel open lifetime is a linear function of $[Mg^{2+}]_{ex}$, with a slope equal to k_{+Mg} (Fig. 1 C). Mg^{2+} unbinding, either by dissociation back to the extracellular solution or permeation through the channel, relieves the block. We define the sum of k_{-Mg} and k_{pMg} to be k_{off}, which is the net rate for Mg^{2+} release from the pore.

According to this model, the equilibrium dissociation constant for Mg^{2+} ($K_{d,Mg}$) is defined as the ratio of the "off" rate and the association rate constant:

$$K_{d,Mg} = \frac{k_{-Mg} + k_{pMg}}{k_{+Mg}} = \frac{k_{off}}{k_{on}}.$$

In the following studies, k_{+Mg}, k_{-Mg}, and k_{pMg} were estimated as a function of the concentration of permeant ions (Na^+ or K^+). Throughout, we use k to represent the apparent rate constant for Mg^{+2} block in the presence of permeant ions, and the Greek letter κ for the corresponding rate constant in the absence of competing ions.

Fitting, Simulations, and Statistics

Fits and simulations were made using MICROCAL ORIGIN (version 4.0; Microcal Software) and SCIENTIST (version 2.0; MicroMath Scientific Software). In SCIENTIST, the comparison of the models having different numbers of free parameters was carried out using the Model Selection Criterion (MSC):

$$\text{MSC} = \ln\frac{\sum_{i=1}^{n}(Y_{obs_i} - \hat{Y}_{obs})^2}{\sum_{i=1}^{n}(Y_{obs_i} - Y_{cal_i})^2} - \frac{2p}{n},$$

where n is the number of points, p is the number of free parameters, and $\hat{Y}_{obs}$ is the mean of the observed data. The MSC will give the same ranking as the Akaike Information Criterion, but is normalized so that it is independent of the scaling of the data points. The most appropriate model, regardless of the number of free parameters, is the one with the largest MSC.

The number of intervals in each open or closed duration histogram was ~1,000. Each symbol in the figures is the mean ± SD of from three to seven patches. In most cases, the SD was smaller than the size of the symbol and is not visible.

RESULTS

Extracellular Na^+ Decreases the Mg^{2+} Association Rate Constant in a Voltage-independent Manner

Fig. 2 A illustrates the effects of extracellular Na^+ on Mg^{2+} association. At higher extracellular Na^+ concentrations ($[Na^+]_{ex}$) openings are longer, indicating a reduced rate of Mg^{2+} association. In Fig. 2 B the inverse open channel lifetime is plotted as a function of $[Mg^{2+}]_{ex}$ for different $[Na^+]_{ex}$. The slope of this relationship, which is the apparent Mg^{2+} association rate constant, is nearly five times slower in 150 mM $[Na^+]_{ex}$ compared with 50 mM $[Na^+]_{ex}$.

We next examined the voltage dependence of the inhibition of Mg^{2+} association by extracellular [Na^+] using the relationship:

$$k^V_{+Mg} = k^0_{+Mg}e^{\psi V}, \quad (1)$$

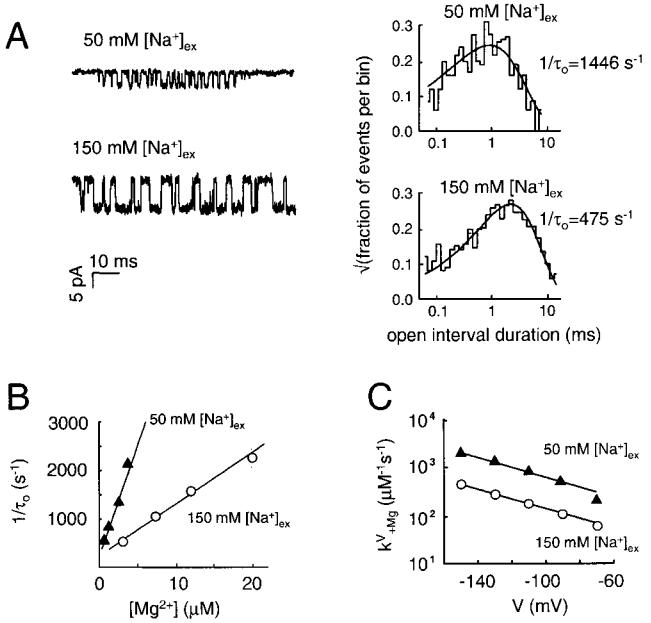

FIGURE 2. Effects of extracellular Na^+ on the Mg^{2+} association rate constant. (A, left) Single-channel currents recorded at different $[Na^+]_{ex}$ ($[Mg^{2+}]_{ex}$ = 3 μM, $[Na^+]_{in}$ = 5 mM; V = −80 mV). (A, right) Open interval duration distributions. Open intervals are longer (i.e., block by Mg^{2+} is slower) at higher $[Na^+]_{ex}$. (B) The inverse open channel lifetime ($1/\tau_o$) versus $[Mg^{2+}]_{ex}$. Increasing extracellular $[Na^+]$ reduces the slope (which is equal to the Mg^{2+} association rate constant) about fivefold, from 500.0 ± 35.6 $\mu M^{-1}s^{-1}$ in 50 mM $[Na^+]_{ex}$ to 109.6 ± 6.9 $\mu M^{-1}s^{-1}$ in 150 mM $[Na^+]_{ex}$. (C) The Mg^{2+} association rate constant versus membrane potential, at different $[Na^+]_{ex}$. The solid line is the fit by Eq. 1. The apparent voltage dependence of the Mg^{2+} association rate constant is the same in 50 mM and 150 mM $[Na^+]_{ex}$ (43 ± 2 mV and 44 ± 1 mV per e-fold change, respectively). In B and C, the SD is smaller than the symbols for all except one point.

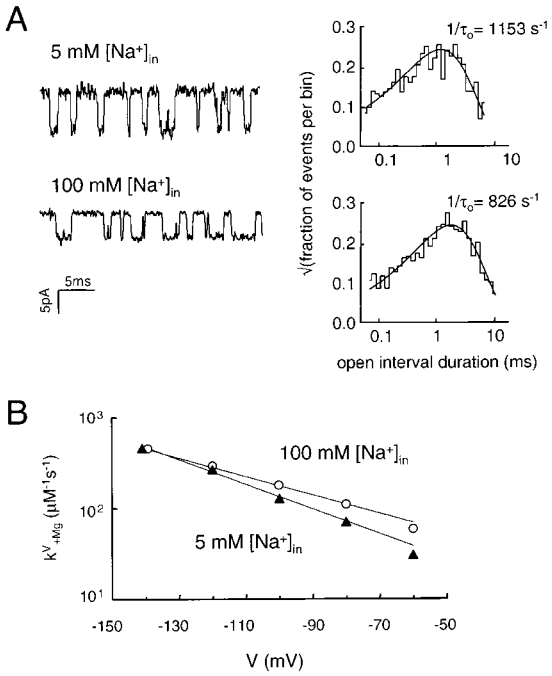

FIGURE 3. Effects of intracellular Na^+ on the Mg^{2+} association rate constant. (A, left) Single-channel currents recorded with different intracellular Na^+ concentrations. The extracellular solution contained 150 mM Na^+ and 7 μM Mg^{2+}, and the membrane potential was −80 mV. (A, right) Open interval duration histograms. Because intracellular Na^+ slows the association of extracellular Mg^{2+}, the inverse of open channel lifetime (τ_o) is faster in 5 mM $[Na^+]_{in}$ (top histogram) than in 100 mM $[Na^+]_{in}$ (bottom histogram). (B) The voltage dependence of the effect of intracellular Na^+ on the Mg^{2+} association rate constant. The apparent Mg^{2+} association rate is plotted against the membrane potential for different $[Na^+]_{in}$. The solid lines are fits by Eq. 1. The inhibition of Mg^{2+} association by $[Na^+]_{in}$ is enhanced by depolarization.

where k^V_{+Mg} is the apparent Mg^{2+} association rate constant at membrane potential V, k^0_{+Mg} is this rate constant in the absence of a membrane potential, and ψ is the apparent voltage dependence of this rate constant (i.e., the inverse of the voltage that elicits an e-fold change). The voltage dependence of k^V_{+Mg} was the same at two different $[Na^+]_{ex}$ (Fig. 2 C), which indicates that the inhibition of the apparent Mg^{2+} association rate constant by extracellular $[Na^+]$ is not voltage-dependent.

Intracellular Na^+ Decreases the Mg^{2+} Association Rate Constant in a Voltage-dependent Manner

Fig. 3 A shows the effects of intracellular Na^+ on Mg^{2+} association. The open channel lifetime is longer at higher $[Na^+]_{in}$, indicating a reduced k_{+Mg}. Fig. 3 B shows that the reduction in k_{+Mg} by $[Na^+]_{in}$ decreases with hyperpolarization, i.e., that $[Na^+]_{in}$ inhibits Mg^{2+} association in a voltage-dependent manner. Using Eq. 1, the apparent voltage dependence of Mg^{2+} association decreases from 44 ± 1 mV per e-fold change in 5 mM $[Na^+]_{in}$, to 32 ± 2 mV per e-fold change in 100 mM $[Na^+]_{in}$.

The Locations and Apparent Affinities of the Na^+ Binding Sites

The effects of $[Na^+]_{ex}$ and $[Na^+]_{in}$ on Mg^{2+} association suggests that these ions compete for positions in the Mg^{2+} association pathway. In the next stage of the analysis, we invoke physically based models that assume that the presence of one or more Na^+ in the permeation pathway substantially reduces or eliminates Mg^{2+} association.

We start with a simple "one-site" scheme to describe the effects of Na^+ on Mg^{2+} association. It is assumed that the Na^+ site is external to, or at the same location as, the Mg^{2+} site, and that extracellular Mg^{2+} can enter and block the channel only when the Na^+ site is empty. Accordingly (see APPENDIX 1), the apparent Mg^{2+} association rate constant (i.e., in the presence of Na^+), k^V_{+Mg}, is a function of three experimental variables ($[Na^+]_{ex}$, $[Na^+]_{in}$, and V) and five free parameters (κ^0_{+Mg}, $K_{Na_{ex}}$, $K_{Na_{in}}$, δ, and α):

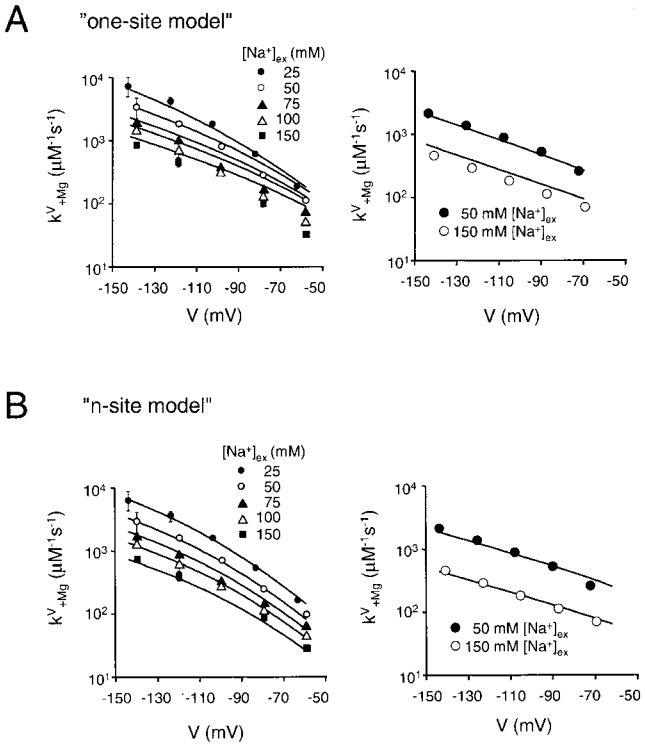

FIGURE 4. Number and affinities of Na^+ binding sites. The Mg^{2+} association rate constant was used to probe the occupancy of the channel by Na^+. Data obtained in 100 mM $[Na^+]_{in}$ are shown to the left, and data obtained in 5 mM $[Na^+]_{in}$ are shown to the right. (A) Fits of experimental Mg^{2+} association rate constants assuming one Na^+ binding site (Eq. 2). The apparent Mg^{2+} association rate constant obtained from different $[Na^+]_{ex}$ is plotted as a function of the membrane potential. A model with a single Na^+ binding site does not provide an adequate description of the experimental results. (B) Fits of the same experimental data by an "n-site" scheme (Eq. 3). The solid lines are the predicted curves from the model (parameters for the best fit are shown in Table I). The model with $n = 2$ independent Na^+ sites is better (MSC = 5.5) than the model with a single Na^+ site (MSC = 4.0).

$$k^V_{+Mg} = \kappa^0_{+Mg} e^{\frac{-2\delta V}{k_B T}} \left(1 + \frac{[Na^+]_{ex}}{K_{Na_{ex}}} + \frac{[Na^+]_{in}}{K^0_{Na_{in}} e^{\frac{-\alpha V}{k_B T}}} \right)^{-1}. \quad (2)$$

k^V_{+Mg} is the Mg^{2+} association rate constant in the absence of competing ions at membrane potential V, and $K_{Na_{ex}}$ and $K^0_{Na_{in}}$ are dissociation constants (k_{off}/k_{on}) for $[Na^+]_{ex}$ and $[Na^+]_{in}$, respectively, with no membrane potential. Note that because Na^+ is a permeant species, these are not equilibrium constants. The two apparent fractional electrical distances in Eq. 2 are δ (between the extracellular compartment to the peak of the entry barrier for Mg^{2+}) and α (between the Na^+ binding site and the intracellular compartment). k_B is Boltzmann's constant, and T is the absolute temperature ($k_BT = 25.3$ mV).

Fig. 4 A shows the result of fitting simultaneously (using Eq. 2) two groups of measurements of k^V_{+Mg} as a function of membrane potential. The first group (Fig. 4 A, left) was obtained from five different $[Na^+]_{ex}$ (25–150 mM) at a single, high $[Na^+]_{in}$ (100 mM). The second group (Fig. 4 A, right) was obtained from two different $[Na^+]_{ex}$ (50 and 150 mM) at a single, low $[Na^+]_{in}$ (5 mM). The curves drawn according to the best fit by Eq. 2 clearly do not describe the experimental data.

Next, we modified the model to incorporate multiple Na^+ binding sites in the channel. We assume that Mg^{2+} can access its site only when all n sites are empty, and, for simplicity, that these sites are identical and independent:

$$k^V_{+Mg} = \kappa^0_{+Mg} e^{\frac{-2\delta V}{k_B T}} \left(1 + \frac{[Na^+]_{ex}}{K_{Na_{ex}}} + \frac{[Na^+]_{in}}{K^0_{Na_{in}} e^{\frac{-\alpha V}{k_B T}}} \right)^{-n}, \quad (3)$$

where n is a free parameter. Fig. 4 B illustrates the fit of the same two groups of experimental data by Eq. 3. The results are given in Table I. A two-site scheme is able to describe the experimental results across Na^+ concentrations and voltages.

Finally, we relaxed the constraint that the two Na^+ binding sites are identical and independent. Eq. 3 was modified to allow different dissociation constants (K_1 and K_2) at each of two distinct Na^+ binding sites:

$$k^V_{+Mg} = \kappa^0_{+Mg} e^{\frac{-2\delta V}{k_B T}} \quad (4)$$

$$\left(1 + \frac{[Na^+]_{ex}}{K_{1,Na_{ex}}} + \frac{[Na^+]_{ex}}{K_{2,Na_{ex}}} + \frac{[Na^+]_{in}}{K^0_{1,Na_{in}} e^{\frac{-\alpha_1 V}{k_B T}}} + \frac{[Na^+]_{in}}{K^0_{2,Na_{in}} e^{\frac{-\alpha_2 V}{k_B T}}} \right)^{-1}.$$

Eq. 4, with eight free parameters, could not be fit to the data (i.e., the SD of the parameters became large). To reduce the number of free parameters, we imposed the constraint of a single voltage dependence term for intracellular Na^+ occupancy (i.e., $\alpha_2 = \alpha_1$). The results are shown in Table I. The fit using the constrained Eq. 4 (MSC = 5.9) was better than using Eq. 3 (MSC = 5.5), indicating that the two Na^+ sites probably are not identical. The apparent dissociation constants differed by 7-fold for extracellular Na^+ (113 ± 35 vs. 15 ± 5 mM) and 3.6-fold for intracellular Na^+ (7.2 ± 5.5 vs. 2.0 ± 0.8 mM). The intrinsic Mg^{2+} association rate constant and fractional electrical distance were similar with Eqs. 3 and 4.

The results indicate that there are at least two Na^+ binding sites in the external portion of the ion permeation pathway that must be empty for Mg^{2+} to associate with the NMDAR pore. Extracellular Na^+ occupies these sites in a nearly voltage-independent manner, whereas intracellular Na^+ occupies these sites in a highly voltage-dependent manner. Na^+ permeates through the channel, thus, this voltage dependence cannot be directly related to a location of the external sites in the electric field.

TABLE I

Na^+ Occupancy and Mg^{2+} Association Rate Constant

Parameter	Symbol	Units	Value	
			Eq. 3	Eq. 4
No. of external sites	n		2.0 ± 0.2	–
Dissociation constant for extracellular Na^+ at the external sites (no Mg^{2+} in the channel)	$K_{Na_{ex}}$	mM	41.8 ± 12.9	113 ± 34.9 15.2 ± 5.1
Dissociation constant for intracellular Na^+ at the external sites (no Mg^{2+} in the channel, no membrane potential)	$K^0_{Na_{in}}$	mM	5.1 ± 2.1	2.0 ± 0.8 7.2 ± 5.5
Fractional electrical distance for Na^+ from intracellular compartment to the external sites	α		0.83 ± 0.07	0.92 ± 0.08
Extracellular Mg^{2+} association rate constant (no competing ions, no membrane potential)	κ^0_{+Mg} ($\times 10^8$)	$M^{-1}s^{-1}$	4.4 ± 0.9	7.8 ± 2.4
Fractional electrical distance for Mg^{2+} from extracellular compartment to the peak of the entry barrier	δ		0.27 ± 0.01	0.24 ± 0.01
Goodness of fit	MSC		5.50	5.90

$K_{Na_{ex}}$ and $K^0_{Na_{in}}$ are apparent (nonequilibrium) dissociation constants (k_{off}/k_{on}) for Na^+ arising from the extracellular and intracellular compartments, respectively, with no Mg^{2+} in the pore. MSC is the Model Selection Criterion, with the higher number indicating the better fit (after accounting for the different in the number of free parameters; see MATERIALS AND METHODS).

This analysis provides information on the intrinsic rate constant of Mg^{2+} association in pure water (i.e., in the absence of competing ions). The association rate constant for extracellular Mg^{2+} is very high ($>10^8$ $M^{-1}s^{-1}$), even in the absence of a membrane potential. The peak of the barrier of the Mg^{2+} association rate constant is located ~25% through the electric field from the extracellular surface.

Extracellular Na^+ Reduces the Mg^{2+} Dissociation Rate Constant

A bound Mg^{2+} has two routes by which it can exit the channel. It can either dissociate back into the extracellular compartment (rate constant k^V_{-Mg}) or it can permeate into the intracellular compartment (rate constant k^V_{pMg}). Both of these processes may be influenced by the presence of Na^+ in the permeation pathway, and such effects are of interest insofar as they provide infor-

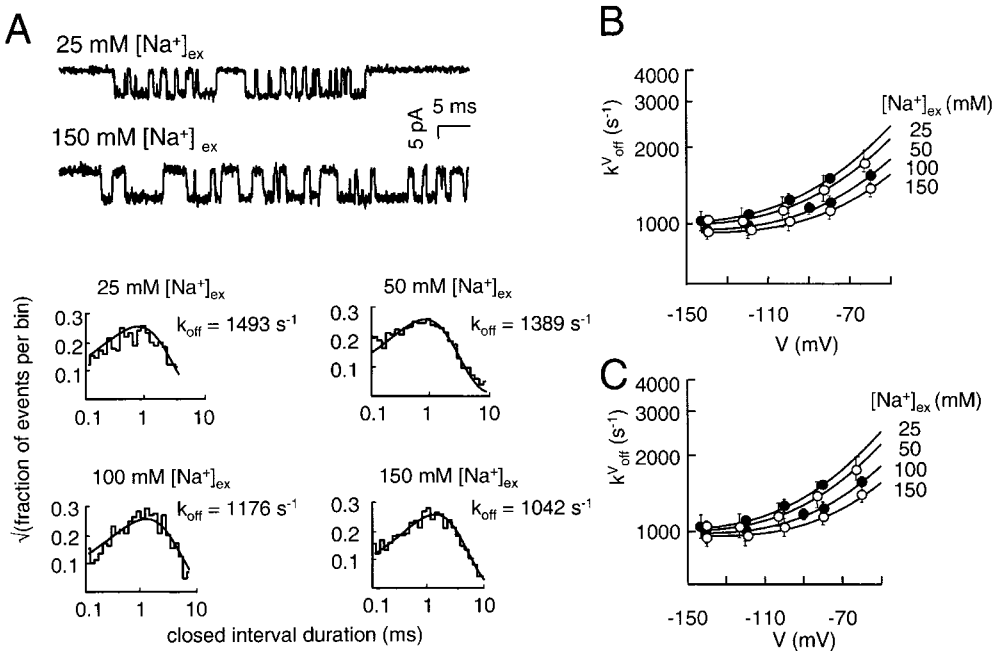

FIGURE 5. Effect of extracellular Na^+ on the Mg^{2+} off rate constant. (A) Single-channel currents of Mg^{2+} block recorded with different extracellular Na^+ concentrations (5 μM extracellular Mg^{2+}, 5 mM $[Na^+]_{in}$, V = −80 mV). Closed interval duration histograms are shown below. The Mg^{2+} off rate decreases with increasing $[Na^+]_{ex}$. (B) Separating the Mg^{2+} off rate into a dissociation rate constant and a permeation rate constant. The solid lines are the fits using Eq. 4. Each point is the mean ± SD of at least three patches (SD may be smaller than the symbol). (C) Analyses of the inhibition of the Mg^{2+} dissociation rate constant by extracellular Na^+. The same four sets of data as in B were fitted simultaneously by Eq. 5. The solid lines are the predicted curves from the model. The parameters are κ^0_{-Mg} = 8,944 ± 205 s^{-1}, ε = 0.36 (fixed), k^0_{pMg} = 624 ± 5 s^{-1}, λ = 0.03 (fixed), and $K_{Na_{ex}}$ = 251 ± 12 mM. Additional results are summarized in Table III and Fig. 6.

mation about the location of the Na^+ binding sites with respect to the Mg^{2+} site.

Only the sum of the exit rate constants, k^V_{off}, can be measured directly from the duration of the blocking gaps in the single-channel current record. However, because the exit routes require Mg^{2+} to move in opposite directions in the electric field, k^V_{-Mg} and k^V_{pMg} will have opposite voltage dependencies, the former decreasing and the latter increasing with hyperpolarization. Using the standard barrier framework, the apparent exit rate constants can be estimated using the relationships:

$$\begin{aligned} k^V_{off} &= k^V_{-Mg} + k^V_{pMg} \\ k^V_{-Mg} &= k^0_{-Mg} e^{\frac{2\varepsilon V}{k_B T}} \\ k^V_{pMg} &= k^0_{-Mg} e^{\frac{-2\lambda V}{k_B T}}, \end{aligned} \tag{5}$$

where k^0_{-Mg} and k^0_{pMg} are the apparent exit rate constants in the absence of a membrane potential, ε is the fractional electrical distance from the Mg^{2+} binding site to the peak of the dissociation barrier, and λ is the fractional electrical distance from the binding site to the peak of the permeation barrier (see Fig. 6).

Fig. 5 A shows single-channel currents and interval duration histograms at different extracellular Na^+ concentrations. The lifetime of the blocked state increases with an elevation of $[Na^+]_{ex}$. This suggests that extracellular Na^+ inhibits Mg^{2+} dissociation from the channel ("lock-in"). Fig. 5 B shows that similar effects were observed over a wide range of membrane potentials. For each $[Na^+]_{ex}$, both k^V_{-Mg} and k^V_{pMg} were estimated by fitting k_{off} versus membrane potential by Eq. 5. Because the occupancy of the Na^+ sites by extracellular Na^+ is voltage-independent, in this procedure, we assumed that the effect of $[Na^+]_{ex}$ on the Mg^{2+} exit rate constants was also voltage-independent (i.e., ε and λ were assumed to be constants).

The results (Fig. 5 B and Table II) show that Mg^{2+} dissociation to the extracellular solution decreases with increasing $[Na^+]_{ex}$. This suggests that occupancy of an external site(s) by Na^+ reduces significantly the rate of Mg^{2+} dissociation to the extracellular compartment. This lock-in effect is consistent with the notion that Na^+ exerts its effects on Mg^{2+} association and dissociation by binding to specific sites in the ion permeation pathway rather than by acting via a nonspecific charge screening mechanism. Moreover, the lock-in effect indicates that Na^+ binds to one or more sites that are distinct from, and extracellular to, the Mg^{2+} binding site. There was no significant effect of extracellular Na^+ on the Mg^{2+} permeation rate constant.

The inhibition of Mg^{2+} dissociation by extracellular Na^+ was analyzed using a model in which Mg^{2+} can dissociate back to the extracellular solution only when all

TABLE II

The Effects of Extracellular $[Na^+]$ on Mg^{2+} Dissociation and Permeation

	k^0_{-Mg}	ε	k^0_{pMg}	λ
	s^{-1}		s^{-1}	
$[Na^+]_{ex}$ = 25 mM	6,909 ± 1,888	0.36 ± 0.08	675 ± 288	0.03 ± 0.03
$[Na^+]_{ex}$ = 50 mM	5,860 ± 1,259	–	671 ± 283	–
$[Na^+]_{ex}$ = 100 mM	4,417 ± 760	–	650 ± 262	–
$[Na^+]_{ex}$ = 150 mM	3,513 ± 480	–	645 ± 249	–

k^0_{-Mg} is the rate constant for Mg^{2+} dissociation from the pore to the extracellular solution, and k^0_{pMg} is the rate constant for Mg^{2+} permeation into the intracellular solution in the absence of a membrane potential. The dissociation rate constant decreases as extracellular $[Na^+]$ increases because a bound Mg^{2+} cannot return to the extracellular solution when Na^+ occupies an external binding site. ε is the electrical distance from the Mg^{2+} binding site to peak of the dissociation barrier, and is λ the electrical distance to the peak of the permeation barrier (see Fig. 6). We assume that these values do not change with the extracellular $[Na^+]$. The values (±SD) were obtained by fitting Eq. 4 globally (i.e., simultaneously to multiple data sets) to the data shown in Fig. 5 B.

of the external Na^+ sites are empty. Accordingly (APPENDIX 2), k^V_{off} is a function of $[Na^+]_{ex}$ and V:

$$k^V_{off,\,Mg} = \kappa^0_{-Mg} e^{\frac{2\varepsilon V}{k_B T}} \left(1 + \frac{[Na^+]_{ex}}{J_{d,Na_{ex}}}\right)^{-n} + k^0_{pMg} e^{\frac{-2\lambda V}{k_B T}}. \tag{6}$$

n is the number of (independent and identical) sites that must be occupied to lock-in the Mg^{2+}, κ^V_{-Mg} is the Mg^{2+} dissociation rate constant when all of the salient external Na^+ sites are empty at membrane potential V, and $J_{d,Na_{ex}}$ is the equilibrium dissociation constant of $[Na^+]_{ex}$ for each Na^+ site, and is assumed to be independent of the membrane potential. Note that $J_{d,Na_{ex}}$ is a true equilibrium dissociation constant for Na^+ when there is a Mg^{2+} in the pore, whereas $K_{Na_{ex}}$ is an apparent dissociation constant for extracellular Na^+ when the pore does not contain a Mg^{2+}.

Four sets of experimental data were fitted by Eq. 6, either with n as a fixed parameter (equal to 1 or 2) or as a free parameter. ε and λ were fixed at their previously determined values (0.36 and 0.03, respectively), leaving only κ^0_{-Mg}, $J_{d,Na_{ex}}$, and k^0_{pMg} as free parameters. The predicted curves match the experimental results (Fig. 5 C), with the best-fit parameters shown in Table III. The results indicate that a model having a single Na^+ site (with an equilibrium dissociation constant of 88 mM), or one with two independent Na^+ sites (each with an equilibrium dissociation constant of 251 mM) can account for the results. In pure water, the Mg^{2+} dissociation rate constant is ~9,000 s^{-1}, and the Mg^{+2} permeation rate constant is 624 s^{-1}.

DISCUSSION

The rate constants of Mg^{2+} block and unblock determined from single-channel kinetic analysis were used to report on the steady-state occupancy of the recombi-

TABLE III

Na^+ Equilibrium Binding and Mg^{2+} Dissociation and Permeation

Parameter	Symbol	Units			
No. of external sites	n		1 (fixed)	2 (fixed)	1.3 ± 0.5
Equilibrium dissociation for extracellular Na^+ at the external site (Mg^{2+} present in the channel)	$J_{d,Na_{ex}}$	mM	88.5 ± 5.6	251 ± 12	129 ± 86.3
Mg^{2+} dissociation rate constant (no competing ions, no membrane potential)	κ^0_{-Mg}	s^{-1}	9,641 ± 277	8,944 ± 205	9,318 ± 86.3
Mg^{2+} permeation rate constant (no competing ions, no membrane potential)	κ^0_{pMg}	s^{-1}	623 ± 4.8	624 ± 5.0	624 ± 5.0
Goodness of fit	MSC		4.97	4.95	4.89

The results were obtained by fitting to Eq. 5 assuming one or two (equal) external sites. The electrical distances (see Fig. 6) ε (0.36; Mg^{2+} binding site to the extracellular compartment) and λ (0.03; Mg^{2+} binding site to the intracellular compartment) were fixed to their values obtained by fitting with Eq. 4 (Table II).

nant NR1-NR2A NMDAR permeation pathway by Na^+. The framework for the analyses was the "Woodhull" formalism (Hille, 1992) using a two (asymmetric) barrier, 1-well model that attributes all of the voltage dependence to the movement of the ion through the electric field. Such a simple scheme is probably a reasonable approximation for ions that have long, exponentially distributed lifetimes in the pore, such as Mg^{2+} and Ca^{2+}. However, it is unclear whether or not this simple framework can be used to approximate the free energy profile for a highly mobile species such as Na^+. Moreover, it is reasonable to suspect that the ionic environment and/or voltage can deform the channel protein to influence Mg^{2+} block and permeation parameters. Nonetheless, we are optimistic that the barrier formalism provides some information about regions of the ion permeation pathway where Na^+ lingers during its brief sojourn in the NMDAR channel.

Changes in the Mg^{2+} parameters as a function of the intra- and extracellular Na^+ concentrations were interpreted as arising from occupancy of specific sites in the ion permeation pathway by the monovalent ion. Because the ionic strength was not constant, it is also possible that some of the effects can be attributed to different degrees of surface charge. Several results lead us to suspect that charge screening was not a major factor. First, the magnitudes of the observed changes in k_{+Mg} are greater than those predicted by charge-screening effects alone. In native hippocampal NMDAR, a reduction in extracellular Cs^+ from 150 to 10 mM creates an excess local negative potential of ~6.5 mV (Zarei and Dani, 1994), which would be expected to increase k_{+Mg} only $e^{6.5/12.5} = 1.7$-fold. We observe a 4.6-fold increase in this rate constant between 150 and 50 mM extracellular Na^+ (Fig. 2). Second, increasing the intracellular Na^+ concentration reduces the apparent association rate constant for extracellular Mg^{2+} in a voltage-dependent manner, which is not predicted by a simple charge-screening mechanism. Third, the difference in the apparent affinity of the external sites for extracellular Na^+ versus K^+ (see Zhu and Auerbach, 2001, in this issue) suggests specific binding rather than a nonspecific surface charge effect. Fourth, the ability of extracellular Na^+ to prevent Mg^{2+} dissociation (the lock-in effect; Table II) is more consistent with occupancy of a binding site than with a charge screening mechanism. Overall, the results suggest that monovalent cations exert their effects on Mg^{2+} association and dissociation predominantly by binding to specific sites in the ion permeation pathway rather than by acting via a nonspecific electrostatic shielding mechanism.

The Na^+ Binding Sites

The results suggest that occupancy of either of the two external sites by Na^+ (arising from the extracellular or the intracellular compartment) slows or prevents Mg^{2+} entry into the channel from the extracellular solution. When the pore is free from Mg^{2+}, extracellular Na^+ binding is voltage-independent, whereas intracellular Na^+ binding is strongly voltage-dependent. When the pore is blocked by Mg^{2+}, a voltage-independent occupancy of a single external site by Na^+ is sufficient to prevent Mg^{2+} dissociation to the extracellular compartment, but is without effect on Mg^{2+} permeation.

In unblocked NMDAR, the voltage sensitivities of the Na^+ effect cannot be used to pinpoint the locations of the external sites in the electric field because we do not know the extent to which Na^+ release is determined by its dissociation back to the extracellular solution versus permeation. If dissociation dominates, then the voltage independence of the dissociation constant for extracellular Na^+ would indicate that both sites lie near or beyond the external margin of the electric field. However, if Na^+ release is predominantly determined by its permeation to the intracellular compartment, the voltage sensitivities would suggest that at least one of the external sites is located deep in the pore. Under this condition, Na^+ occupancy of a deep site would show a reduced voltage dependence because the on and off rates to the site will change in the same direction with a change in the membrane potential. The apparent voltage dependence of occupancy would disappear if the electrical distance

from the site to the peak of the permeation barrier was similar to that from the extracellular solution to the entry barrier (i.e., $\delta \approx \alpha$, for Na^+). At the same time, intracellular Na^+ occupancy of that site would exhibit a steep voltage dependence because the on and off rates would change in opposite directions with voltage.

Our results do not allow us to unequivocally pinpoint the locations of the Na^+ sites. Some results point to a separation of the Na^+ sites, with one external Na^+ site located near or beyond the extracellular margin of the electrical field and the other being close to, or perhaps the same as, the Mg^{2+} site (which is 0.6 though the electric field). First, the higher apparent affinity of the external sites for intracellular (compared with extracellular) Na^+ suggests that the barrier to Na^+ dissociation to the external compartment is higher than the Na^+ permeation barrier. Thus, Na^+ release is likely to be dominated by permeation. Second, although occupancy of either of two external sites prevents Mg^{2+} association, the results are consistent with a scheme in which only a single site must be occupied to prevent Mg^{2+} dissociation to the extracellular solution. The occupancy of this lock-in site for Na^+ is not voltage-dependent. Because this affinity constant is determined under equilibrium conditions (i.e., no permeation), this indicates that this site lies near or beyond the extracellular boundary of the electric field. These arguments are not definitive, and the existence of two nonidentical Na^+ sites near or beyond the extracellular limit of the electric field remains a possibility.

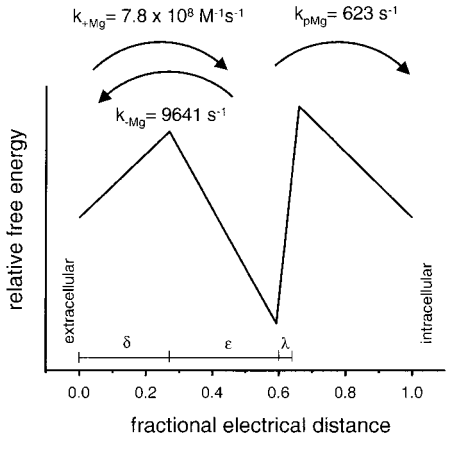

FIGURE 6. Energy profile for Mg^{2+} block and permeation. The rate constants pertain to extracellular Mg^{2+} in pure water (no competing ions) and with no membrane potential. The fractional electrical distances are indicated below, where δ pertains to the Mg^{2+} entry barrier (= 0.25), ε pertains to the Mg^{2+} dissociation (= 0.35), and λ pertains to the Mg^{2+} permeation barrier (= 0.03). The Mg^{2+} binding site is 0.60 through the electric field from the extracellular solution.

Mg^{2+} Block in Pure Water

The intrinsic parameters for Mg^{2+} binding to the NMDAR pore, i.e., in the absence of competing permeant ions, are shown in Fig. 6. In pure water and no membrane potential, the association rate constant for extracellular Mg^{2+} is 7.8×10^8 $M^{-1}s^{-1}$. This is 100 times faster than the apparent association rate constant in 140 mM extracellular Na^+. The large magnitude of this rate constant indicates that, in the absence of competing ions, Mg^{2+} has unhindered access to its blocking site in the channel.

In pure water and no membrane potential, Mg^{2+} exits the NMDAR pore mainly by dissociating to the extracellular solution (at $\sim$9,000 s^{-1}), but it can also permeate into the intracellular compartment (at 62 s^{-1}). Thus, under these conditions, Mg^{2+} stays in the pore $\sim$0.1 ms and $\sim$6.5% of the blocking events results in the permeation of a Mg^{2+}. The Mg^{2+} permeation rate constant is slow and predicts that this ion can carry only a tiny current ($\sim$0.2 fA) that would normally be an insignificant fraction of the total single-channel current. From the rate constants, we estimate that in the absence of competing ions and at zero membrane potential, the intrinsic equilibrium dissociation constant of the NMDAR for Mg^{2+} is $\sim$12 μM.

The main barrier to Mg^{2+} association is located 0.25 through the electric field (i.e., this process increases e-fold with a 46-mV hyperpolarization). At -60 mV, the Mg^{2+} association rate constant in pure water is $\sim 2.2 \times 10^9$ $M^{-1}s^{-1}$. The entry barrier appears to be nearly symmetric, as a bound Mg^{2+} must traverse 0.35 of the field to return to the extracellular compartment (35 mV for an e-fold change). The sum of these two positional parameters indicates that the Mg^{2+} binding site is located 0.6 through the electric field from the extracellular solution. In contrast, the barrier to Mg^{2+} permeation is very steep, as the ion, once bound, must traverse only 0.03 of the field to reach the intracellular compartment. Thus, hyperpolarization has very little effect on Mg^{2+} permeation, per se, whereas it significantly speeds the association from, and slows the dissociation of Mg^{2+} to, the extracellular solution.

In the absence of competing ions, equilibrium block by Mg^{2+} increases e-fold with a hyperpolarization of $\sim$21 mV, so that at -60 mV, the Mg^{2+} equilibrium dissociation constant is only $\sim$0.7 μM. Under these conditions, almost one out of every three Mg^{2+} that binds permeates through the channel.

Comparison with Native NMDARs

There have been several excellent studies of the effects of extracellular Na^+ and intracellular Cs^+ on block of native NMDAR (embryonic rat cortical neurons, probably composed of a mixture of NR2A and B subunits)

by adamantine derivatives (Antonov et al., 1998) and Mg^{2+} (Antonov and Johnson, 1999). For the most part, our results using recombinant NMDARs are in good agreement with these studies. Both sets of results show that extracellular Na^+ binds to two sites (average $K_{Na_{ex}} = \sim$40 mM) that are in the external portion of the channel to thereby prevent the entry of Mg^{2+} into the pore. In addition, both sets of results show a lock-in effect, i.e., that the occupancy of either site prevents Mg^{2+} dissociation back to the extracellular solution. Our results also agree with those of Antonov and Johnson (1999) with respect to the intrinsic parameters for Mg^{2+} association. Both sets of results indicate a similar electrical distance of the association barrier from the extracellular solution (0.25 vs. 0.23) and a large association rate constant at zero potential in pure water ($\sim$8 vs. 11 $\times$ 10^8 $M^{-1}s^{-1}$).

Our measurements indicate that the intrinsic Mg^{2+} dissociation rate constant is $\sim$10 times slower, and that the Mg^{2+} permeation rate constant is $\sim$10 times faster than was reported by Antonov and Johnson (1999). As a consequence, we estimate a higher intrinsic affinity (in pure water and the absence of a membrane potential) of the pore for extracellular Mg^{2+} (12 vs. 101 μM). Moreover, our estimate of the location (in electrical distance) of the Mg^{2+} binding site (0.60) is different from that of Antonov and Johnson (0.47). We doubt that these differences arise from a different subunit composition of recombinant (NR2B) versus native systems (NR2A and NR2B). Rather, we speculate that these differences arise from the fact that they used 130 mM Cs^+ in their intracellular solution, whereas we used 5 mM Na^+. Occupancy of an internal monovalent cation-binding site by Cs^+ will increase the apparent rate constant for Mg^{2+} dissociation and slow the apparent rate constant for Mg^{2+} permeation (see Zhu and Auerbach, 2001, in this issue).

Mg^{2+} Block and Unblock as a Function of the Na^+ Concentrations and the Membrane Potential

Eqs. 4 and 5 can be combined to describe Mg^{2+} block kinetics as a function of $[Na^+]$ and the membrane potential (in the absence of other competing ions). Using the parameters shown in Tables I and III, at −60 mV and under the conditions $[Na^+]_{ex}$ = 140 mM and $[Na^+]_{in}$ = 10 mM, the apparent Mg^{2+} block and unblock rates are, respectively, 2 $\times$ 10^8 $M^{-1}s^{-1}$ and 1,270 s^{-1}, with about equal probabilities of release to the extra- and intracellular compartments, yielding an apparent K_d of $\sim$0.6 mM. These conditions are not "physiological" because they do not incorporate the effects of K^+, which is present at a high concentration in the intracellular compartment. In the companion paper (see Zhu and Auerbach, 2001, in this issue) we describe the effects of extra- and intracellular K^+ on the kinetics of Mg^{2+} blockade.

APPENDIX 1

We assume that (1) there is a single Na^+ binding site; (2) Mg^{2+} can bind to the channel only when this site is empty; and (3) the Na^+ association and dissociation rate constants are much faster than the Mg^{2+} association rate constant. Thus,

$$k^V_{+Mg} = \kappa^0_{+Mg} P^e_{Na}, \qquad \text{A1.1}$$

where k^V_{+Mg} is the apparent Mg^{2+} association rate constant at membrane potential V, (i.e., in the presence of Na^+), k^V_{+Mg} is the Mg^{2+} association rate constant in pure water at membrane potential V, and P^e_{Na} is the probability of the Na^+ site being empty. P^e_{Na} is a function of the equilibrium dissociation constants and ion concentrations:

$$P^e_{Na} = \left(1 + \frac{[Na^+]_{ex}}{K_{Na_{ex}}} + \frac{[Na^+]_{in}}{K^V_{Na_{in}}}\right)^{-1}, \qquad \text{A1.2}$$

where $K_{Na_{ex}}$ and $K^V_{Na_{in}}$ are the unidirectional dissociation constants (k_{off}/k_{on}) for $[Na^+]_{ex}$ and $[Na^+]_{in}$, respectively. k^V_{+Mg} is related to the membrane potential by:

$$\kappa^V_{+Mg} = \kappa^0_{+Mg} e^{\frac{-2\delta V}{k_B T}}, \qquad \text{A1.3}$$

where κ^0_{+Mg} is the Mg^{2+} association rate constant in the absence of a membrane potential, δ is the fractional electrical distance between the extracellular compartment and the peak of the entry barrier for Mg^{2+}, k_B, is the Boltzmann constant, and T is the absolute temperature (under our conditions, k_BT = 25.3 mV). We assume that $K_{Na_{ex}}$ is voltage-independent (Fig. 2 C), and that $K^V_{d,Na_{in}}$ is voltage-dependent (Fig. 3 C) and is related to the membrane potential by:

$$K^V_{Na_{in}} = K^0_{Na_{in}} e^{\frac{-\alpha V}{k_B T}}, \qquad \text{A1.4}$$

where $K^0_{Na_{in}}$ is the intracellular Na^+ equilibrium dissociation constant at zero membrane potential, and α is the fractional electrical distance of the Na^+ site from the intracellular solution. We now generate a description of k^V_{+Mg} as a function of three experimental variables ($[Na^+]_{ex}$, $[Na^+]_{in}$, and V) and five free parameters (κ^0_{+Mg}, $K_{d,Na_{ex}}$, $K_{d,Na_{in}}$, δ, and α):

$$k^V_{+Mg} = \kappa^0_{+Mg} e^{\frac{-2\delta V}{k_B T}} \left(1 + \frac{[Na^+]_{ex}}{K_{Na_{ex}}} + \frac{[Na^+]_{in}}{K^0_{Na_{in}} e^{\frac{-\alpha V}{k_B T}}}\right)^{-1}. \qquad \text{A1.5}$$

APPENDIX 2

We assume that there are n identical and independent Na^+ binding sites that must be empty for Mg^{2+} to dissociate back to the extracellular compartment. The apparent Mg^{2+} dissociation rate (i.e., in the presence of extracellular Na^+) is:

$$k^{V}_{-Mg} = \kappa^{V}_{-Mg}(P^{e}_{Na})^{n}, \quad \text{A2.1}$$

where κ^{V}_{-Mg} is the Mg^{2+} dissociation rate constant in pure water at membrane potential V and P^{e}_{Na} is the probability that all of the Na^{+} sites are empty. Because intracellular Na^{+} cannot reach the external site(s) when Mg^{2+} is bound, Eq. A1.2 was modified so that P^{e}_{Na} depends only on $[Na]_{ex}$:

$$P^{e}_{Na} = \left(1 + \frac{[Na^{+}]_{ex}}{J_{d,Na_{ex}}}\right)^{-1}, \quad \text{A2.2}$$

where $J_{d,Na_{ex}}$ is the equilibrium dissociation constant of $[Na^{+}]_{ex}$ for each Na^{+} site and is assumed to be independent of the membrane potential. Note that $J_{d,Na_{ex}}$ is a true equilibrium dissociation constant for Na^{+} when there is a Mg^{2+} in the pore, whereas $K_{Na_{ex}}$ is an apparent (nonequilibrium) dissociation constant for Na^{+} when the pore does not contain a Mg^{2+}.

We now describe k^{V}_{-Mg} as a function of $[Na^{+}]_{ex}$ and V:

$$k^{V}_{-Mg} = \kappa^{0}_{-Mg} e^{\frac{-2\varepsilon V}{k_B T}} \left(1 + \frac{[Na^{+}]_{ex}}{J_{d,Na_{ex}}}\right)^{-n}. \quad \text{A2.3}$$

and k^{V}_{off} as a function of the experimental variables $[Na^{+}]_{ex}$ and V:

$$k^{V}_{off} = \kappa^{0}_{-Mg} e^{\frac{2\varepsilon V}{k_B T}} \left(1 + \frac{[Na^{+}]_{ex}}{J_{d,Na_{ex}}}\right)^{-2} + k^{0}_{pMg} e^{\frac{-2\lambda V}{k_B T}}. \quad \text{A2.4}$$

We thank Thomas Kuner and Peter Seeburg for the rat NR1 and NR2A subunit cDNAs, and Jon Johnson for insightful comments on the manuscript.

This work was supported by a grant to A. Auerbach (NS-86554).

Submitted: 26 May 2000
Revised: 24 January 2001
Accepted: 25 January 2001

REFERENCES

Antonov, S.M., and J.W. Johnson. 1999. Permeation ion regulation of N-methyl-D-aspartate receptor channel block by Mg^{2+}. *Proc. Natl. Acad. Sci. USA.* 96:14571–14576.

Antonov, S.M., V.E. Gimiro, and J.W. Johnson. 1998. Binding sites for permeant ions in the channel of NMDA receptors and their effects on channel block. *Nat. Neurosci.* 1:451–461.

Ascher, P., and L. Nowak. 1988. The role of divalent cations in the N-methyl-D-aspartate responses of mouse central neurones in culture. *J. Physiol.* 399:247–266.

Asztely, F., and B. Gustafsson. 1996. Ionotropic glutamate receptors: their role in the expression of hippocampal synaptic plasticity. *Mol. Neurobiol.* 12:1–11.

Barry, P.H., and J.W. Lynch. 1991. Liquid junction potentials and small cell effects in patch-clamp analysis. *J. Membr. Biol.* 121:101–117.

Burnashev, N., R. Schoepfer, H. Monyer, J.P. Ruppersberg, W. Gunther, P.H. Seeburg, and B. Sakmann. 1992. Control by asparagine residues of calcium permeability and magnesium blockade in the NMDA receptor. *Science.* 257:1415–1419.

Burnashev, N., Z. Zhou, E. Neher, and B. Sakmann. 1995. Fractional calcium currents through recombinant GluR channels of the NMDA, AMPA and kainate receptor subtypes. *J. Physiol.* 485: 403–418.

Chen, H.S., and S.A. Lipton. 1997. Mechanism of memantine block of NMDA-activated channels in rat retinal ganglion cells: uncompetitive antagonism. *J. Physiol.* 499:27–46.

Chung, S.H., J.B. Moore, L.G. Xia, L.S. Premkumar, and P.W. Gage. 1990. Characterization of single channel currents using digital signal processing techniques based on hidden Markov models. *Proc. R. Soc. Lond. B.* 329:265–285.

Cull-Candy, S.G., and M.M. Usowicz. 1987. Multiple-conductance channels activated by excitatory amino acids in cerebellar neurons. *Nature.* 325:525–528.

Hille, B. 1992. Ionic Channels of Excitable Membranes. 2nd edition. Sinauer Associates, Inc., Sunderland, MA. 609 pp.

Iino, M., S. Ozawa, and K. Tsuzuki. 1990. Permeation of calcium through excitatory amino acid receptor channels in cultured rat hippocampal neurones. *J. Physiol.* 424:151–165.

Iino, M, S. Ciani, K. Tsuzuki, S. Ozawa, and Y. Kidokoro. 1997. Permeation properties of Na^{+} and Ca^{2+} ions through the mouse epsilon2/zeta1 NMDA receptor channel expressed in *Xenopus* oocytes. *J. Membr. Biol.* 155:143–156.

Jahr, C.E., and C.F. Stevens. 1990. A quantitative description of NMDA receptor-channel kinetic behavior. *J. Neurosci.* 10:1830–1837.

Jahr, C.E., and C.F. Stevens. 1993. Calcium permeability of the N-methyl-D-aspartate receptor channel in hippocampal neurons in culture. *Proc. Nat. Acad. Sci. USA.* 90:11573–11577.

Maren, S., and M. Baudry. 1995. Properties and mechanisms of long-term synaptic plasticity in the mammalian brain: relationships to learning and memory. *Neurobiol. Learn. Mem.* 63:1–18.

Mayer, M.L., and G.L. Westbrook. 1987. Permeation and block of N-methyl-D-aspartic acid receptor channels by divalent cations in mouse cultured central neurones. *J. Physiol.* 394:501–527.

Mayer, M.L., G.L. Westbrook, and P.B. Guthrie. 1984. Voltage-dependent block by Mg^{2+} of NMDA responses in spinal cord neurones. *Nature.* 309:261–263.

Nowak, L., P. Bregestovski, P. Ascher, A. Herbet, and A. Prochiantz. 1984. Magnesium gates glutamate-activated channels in mouse central neurones. *Nature.* 307:462–465.

Premkumar, L.S., and A. Auerbach. 1996. Identification of a high affinity divalent cation binding site near the entrance of the NMDA receptor channel. *Neuron.* 16:869–880.

Qin, F., A. Auerbach, and F. Sachs. 1996. Estimating single-channel kinetic parameters from idealized patch-clamp data containing missed events. *Biophys. J.* 70:264–280.

Sharma, G., and C.F. Stevens. 1996a. A mutation that alters magnesium block of N-methyl-D-aspartate receptor channels. *Proc. Natl. Acad. Sci. USA.* 93:9259–9263.

Sharma, G., and C.F. Stevens. 1996b. Interactions between two divalent ion binding sites in N-methyl-D-aspartate receptor channels. *Proc. Natl. Acad. Sci. USA.* 93:14170–14175.

Wollmuth, L.P., T. Kuner, and B. Sakmann. 1998. Adjacent asparagines in the NR2-subunit of the NMDA receptor channel control the voltage-dependent block by extracellular Mg^{2+}. *J. Physiol.* 506:13–32.

Zarei, M.M., and J.A. Dani. 1994. Ionic permeability characteristics of the *N*-methyl-D-aspartate receptor channel. *J. Gen. Physiol.* 103: 231–248.

Zhu, Y., and A. Auerbach. 2001. K^{+} occupancy of the *N*-methyl-D-aspartate receptor channel probed by Mg^{2+} block. *J. Gen. Physiol.* 117:287–297.